

VU Research Portal

Switching an Individual Phycobilisome off and on

Gwizdala, Michal; Botha, Joshua L.; Wilson, Adjélé; Kirilovsky, Diana; Van Grondelle, Rienk; Krüger, Tjaart P.J.

published in

Journal of Physical Chemistry Letters
2018

DOI (link to publisher)

[10.1021/acs.jpcllett.8b00767](https://doi.org/10.1021/acs.jpcllett.8b00767)

document version

Publisher's PDF, also known as Version of record

document license

Article 25fa Dutch Copyright Act

[Link to publication in VU Research Portal](#)

citation for published version (APA)

Gwizdala, M., Botha, J. L., Wilson, A., Kirilovsky, D., Van Grondelle, R., & Krüger, T. P. J. (2018). Switching an Individual Phycobilisome off and on. *Journal of Physical Chemistry Letters*, 9(9), 2426-2432.
<https://doi.org/10.1021/acs.jpcllett.8b00767>

General rights

Copyright and moral rights for the publications made accessible in the public portal are retained by the authors and/or other copyright owners and it is a condition of accessing publications that users recognise and abide by the legal requirements associated with these rights.

- Users may download and print one copy of any publication from the public portal for the purpose of private study or research.
- You may not further distribute the material or use it for any profit-making activity or commercial gain
- You may freely distribute the URL identifying the publication in the public portal ?

Take down policy

If you believe that this document breaches copyright please contact us providing details, and we will remove access to the work immediately and investigate your claim.

E-mail address:

vuresearchportal.ub@vu.nl

Switching an Individual Phycobilisome Off and On

Michal Gwizdala,^{*,†,‡} Joshua L. Botha,[‡] Adjélé Wilson,[§] Diana Kirilovsky,[§] Rienk van Grondelle,[†] and Tjaart P. J. Krüger[†]

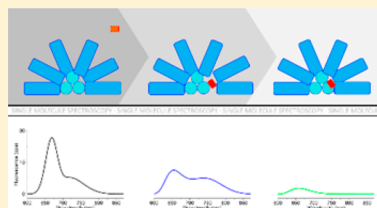
[†]Department of Physics and Astronomy, Faculty of Sciences, VU University, De Boelelaan 1081, 1081 HV Amsterdam, The Netherlands

[‡]Department of Physics, Faculty of Natural and Agricultural Sciences, University of Pretoria, Private bag X20, Hatfield 0028, South Africa

[§]Unité de Recherche Associée 2096, Centre National de la Recherche Scientifique, Service de Bioénergétique, 91191 Gif sur Yvette, France

Supporting Information

ABSTRACT: Photosynthetic organisms have found various smart ways to cope with unexpected changes in light conditions. In many cyanobacteria, the lethal effects of a sudden increase in light intensity are mitigated mainly by the interaction between phycobilisomes (PBs) and the orange carotenoid protein (OCP). The latter senses high light intensities by means of photoactivation and triggers thermal energy dissipation from the PBs. Due to the brightness of their emission, PBs can be characterized at the level of individual complexes. Here, energy dissipation from individual PBs was reversibly switched on and off using only light and OCP. We reveal the presence of quasistable intermediate states during the binding and unbinding of OCP to PB, with a spectroscopic signature indicative of transient decoupling of some of the PB rods during docking of OCP. Real-time control of emission from individual PBs has the potential to contribute to the development of new super-resolution imaging techniques.



The orange carotenoid protein (OCP), phycobilisomes (PBs), and the fluorescence recovery protein (FRP) are the key players in the major photoprotective mechanism in cyanobacteria.¹ By means of molecular mechanisms involving these complexes, the transfer of excitation energy from PBs, the light harvesting complexes of many strains of cyanobacteria, to the photosynthetic reaction centers (RCs) is tightly regulated.^{2,3} These regulatory mechanisms are crucial to sustain the photosynthetic activity despite rapidly fluctuating light conditions.⁴ In particular, when the amount of solar energy absorbed by a PB exceeds the capacity of the RCs, the production of potentially lethal reactive oxygen species in RCs is mitigated by thermal energy dissipation from PB.⁵

In a low light intensity scenario, PBs transfer excitation energy to the RCs. Usually, the absorbed energy flows from six distal phycocyanin (PC) rods to the central core containing bulk allophycocyanin (APC) and the terminal emitters (TEs).^{6–9} The TEs funnel excitations to the RCs.¹⁰ Regulation of the excitation energy flow takes place predominantly in the PB core, either in APC or TE, emitting at ~660 and ~680 nm, respectively.

Besides the regulatory mechanisms present in cyanobacteria occupying extreme conditions,^{11,12} recent single-molecule spectroscopy (SMS) studies on PBs revealed an intrinsic, light-induced energy-dissipative channel that can be activated in any part of PB but with the highest probability at the level of the TEs.¹³ In contrast, the major OCP-related photoprotective mechanism leads to energy quenching at the level of APC.^{14–17}

OCP senses the conditions in which photoprotective energy dissipation is required and, in response, forms an active, red form, known as OCP^r.^{18–21} Under low light intensity conditions, OCP remains in an inactive conformation, characterized by an orange color, and is therefore called OCP^o. Only OCP^r binds to PB^{1,22} and induces excitation energy quenching, i.e., it switches PB's light harvesting functionality off.^{1,4}

WT-OCP (OCP from wild-type *Synechocystis* PCC 6803) does not detach from PB spontaneously, and the energy in PB is quenched as long as an OCP is bound, i.e., as long as FRP does not detach OCP from the PB.^{23–26} When the light intensity decreases, the activity of FRP is signified by the recovery of fluorescence from PB, indicating that PB is switched on again.²³

FRP is not required for the recovery when the positively charged arginine155 in OCP is replaced by an uncharged residue, like leucine.¹⁹ While R155L-OCP induces energy quenching similarly to WT-OCP, it does not form a stable complex with PB.¹⁹ Thanks to its decreased binding affinity to PBs, R155L-OCP is an ideal candidate to study the reversibility of energy quenching in the absence of FRP.

The emission dynamics observed through the lens of SMS provide valuable insight into the fundamental properties of PBs. While these dynamics usually have a stochastic character and

Received: March 12, 2018

Accepted: April 24, 2018

Published: April 24, 2018



can be controlled only to a limited extent, e.g., by alterations in the rate of excitation,¹³ here we present a signature of a controlled interaction between two physiological partners, OCP and PB, revealing biologically relevant phenomena hidden in ensemble measurements.

OCP quenches the excitation energy in PBs upon illumination both in vivo and when isolated in solution. As long as our SMS measurement took place in the dark, i.e., using a laser beam to excite PBs but without any external illumination, we detected an average of 7–8 fluorescing complexes per $10\ \mu\text{m} \times 10\ \mu\text{m}$ region, a number that was independent of the presence of WT-OCP (Figure S1). However, in the presence of WT-OCP and upon short external illumination with a blue light-emitting diode (LED), the average number of clearly visible, strongly fluorescing PB complexes per detection area irreversibly dropped to 0.7 PBs (Figure S1). Moreover, the number of visible, strongly fluorescing complexes did not decrease when immobilized PBs were illuminated with the same blue LED but in the absence of OCP (Figure S2). We can therefore safely conclude that the observed drop in the number of strongly fluorescing complexes in the presence of WT-OCP and upon illumination was due to the formation of stable, quenched OCP–PB complexes.¹ In this experiment, illumination triggered OCP photoactivation, leading to the formation of OCP^r, which bound to the immobilized PB complexes and induced energy dissipation.

In order to investigate the dynamics and molecular characteristics of OCP-induced energy quenching at the level of an individual complex, one PB at a time was excited with a laser beam for a prolonged time of 3 min. Due to the presence of OCP, illumination with the external blue LED triggered energy quenching in the PBs. Figure 1A,B shows two typical examples of PB fluorescence emission traces in the presence of activated WT-OCP, where the decrease in fluorescence intensity was clearly correlated with the external blue LED illumination. The decrease in fluorescence intensity occurred in parallel with shortening of the fluorescence lifetimes, indicating that quenching was caused by energy dissipation and not by pigment bleaching or detachment of a subunit.¹³ The switch into the fully quenched state corresponded to $\sim 90\%$ shortening of the average fluorescence lifetime (down to $0.16 \pm 0.02\ \text{ns}$, vide infra). Once the fluorescence was fully quenched, it remained at a relatively constant level and did not recover throughout the measurement, indicating that WT-OCP remained bound to the PB.

Occasionally, a sudden, large increase in the fluorescence lifetime and a small or negligible change in fluorescence intensity were observed, signifying photodegradation of an OCP–PB complex (Figure S3).¹³ Despite that, the average survival time before photodegradation of the OCP-induced quenched PB complexes was 110 s. Under similar experimental conditions and at a comparable excitation power, the survival time of PBs in the absence of OCP was 23 s.¹³ The nearly 5-fold increase in the survival time in the presence of OCP points to a new possible role of OCP in photoprotection. Apparently, apart from shielding photosynthetic RCs from overexcitation under intensive illumination, OCP also protects and stabilizes the integrity of PBs while in the quenched state. This stabilizing role of OCP may be of particular importance for the emerging in vitro technological applications of OCP.²⁷

Under our experimental conditions, a quenched state lasting longer than a few seconds was observed only rarely, regardless

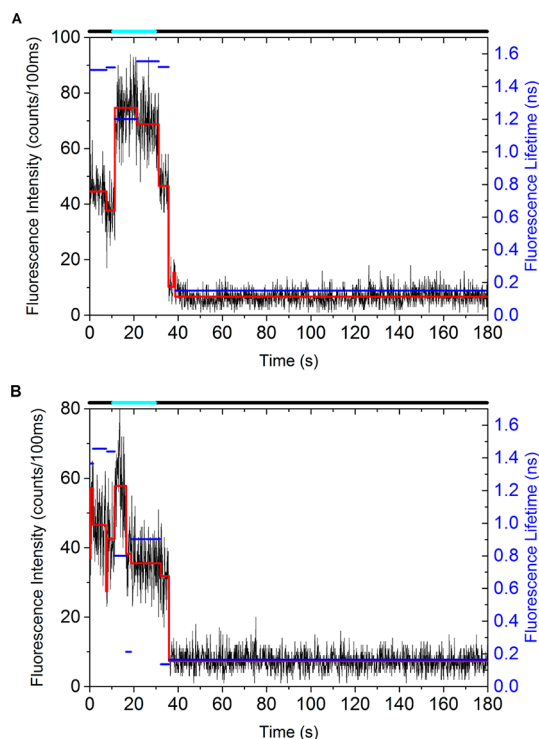


Figure 1. Excitation energy in individual PBs can be quenched using only WT-OCP and light. Representative traces of binned fluorescence counts (black), resolved intensity levels (red), and associated fluorescence lifetimes (blue). The correlated drop in fluorescence intensity and shortening of lifetimes upon 20 s illumination with a blue LED light (cyan bar on top) are caused by accumulation of OCP^r and subsequent binding to PB, inducing irreversible quenching of energy. The LED light increased the detected counts. While in (a) quenching is induced after LED illumination, in (b) quenching is induced during the illumination. The delay time between the start of illumination and quenching depends on diffusion of OCP^r to the PB and is stochastic. Complexes in (a) and (b) remained intact and in a quenched state until the end of the measurement of 180 s. The average dwell time in the fully quenched states from 21 individually measured complexes, characterized by fluorescence lifetimes of $<0.3\ \text{ns}$, was 68 s (SE = 11 s), where “dwell time” denotes the duration of a constant fluorescence intensity level. Laser irradiance of $\sim 0.86\ \text{W}/\text{cm}^2$ at 594 nm was used. Fluorescence lifetimes were fitted for intensity bins of 500 photons or more.

of whether the PBs were in the absence or presence of OCP^o (Figure S4). Analysis of the quenched states observed in the presence of photoactivated WT-OCP^r makes it clear that long-lived quenched states, characterized by an average dwell time of 68 s, are highly unlikely to be observed if the dynamics were purely light-induced, i.e., without OCP. For example, for PB not quenched by OCP, the probability of finding a quenched state lasting between 30 and 120 s is, on average, only 0.4%, while this probability is at least 21% for PB quenched by WT-OCP when using the same excitation rate per complex (Figure S4). The low probability of finding long-lasting quenched states in PB in the absence of OCP, together with correlation between blue LED illumination and the induction of fluorescence quenching in the large majority of measured cases, confirms that the quenched states discussed in this study are related to the activity of OCP. In our experimental setting, OCP^r accumulated due to LED illumination and freely diffused until it eventually bound to PB, inducing a nonemissive state.

Remarkably, induction of a nonemissive state is not a one-step process. Fluorescence spectra, collected concomitantly with the fluorescence lifetimes and intensities, revealed the presence of intermediate states preceding the fully quenched states (Figure 2). The emission in the intermediate states was

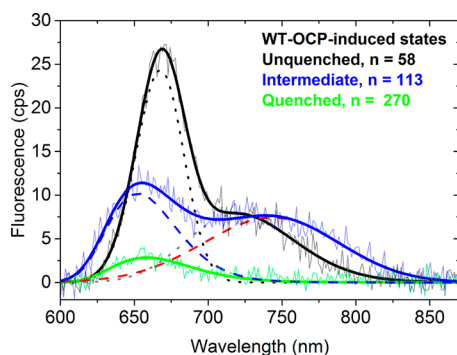


Figure 2. Emission spectra of unquenched, intermediate, and fully quenched states. Measured fluorescence spectra (thin lines) and fits (thick lines) of the unquenched (black) and intermediate (blue) states. Intermediate states occurred between unquenched and fully quenched states. The measured spectra were deconvoluted with two skewed Gaussians with peak positions at 667.7 ± 0.3 (black dotted) and 720.2 ± 4.6 nm (gray dotted) for the unquenched state, and at 652.4 ± 2.0 (blue dashed) and 743.4 ± 5.8 nm (red dashed) for the intermediate states. The red band in the intermediate state spectrum was broad, characterized by a full width at half-maximum (fwhm) of 105 ± 7 nm. Intermediate states are considered those states directly preceding fully quenched states, the latter having fluorescence lifetimes shorter than 0.3 ns. The spectrum of the quenched state (green) was fitted with a skewed Gaussian peaking at 658.5 ± 2.0 nm. The number of spectra, each collected for 1 s, over which each spectrum was averaged is denoted by n . In all cases a measured baseline was subtracted from the spectra.

partly quenched and had excessively broad fluorescence spectra featuring a major peak at 652.4 ± 2.0 nm, on average, further blue-shifted than the average spectral maximum of the fully quenched state at 658.5 ± 2.0 nm. Intuitively, such a large blue shift of an intermediate emission state suggests decreased connectivity between the rods and the core in PBs. Indeed, our modeling confirms that the connectivity should be drastically less; the large spectral shift of the intermediate states can be explained when 2 of the 6 rods, on average, are transiently uncoupled from the PB core or if the average energy-transfer rate between the core and the rods is 20 times lower, or a combination of these two possibilities, such as one rod being fully decoupled and the remaining five having decreased connectivity with the core (Figure 3 and Supporting Modeling). In contrast, the fully quenched states are well-described by the same compartmental kinetic model but with no changes in the rod–core connectivity, i.e., the intercompartmental kinetic energy-transfer rates for intact PB complexes in refs 13 and 15 were used. The average degree of fluorescence quenching (Φ_Q) and extent of the blue shift ($\Delta\lambda_{\max}$) of the measured spectra are presented as two single points in Figure 3, one for the intermediate state (open circle) and one for the fully quenched state (filled circle), and can be compared directly with the modeled relationship between Φ_Q and $\Delta\lambda_{\max}$ for different types of decreased connectivity between the rods and the core. We conclude from Figure 3 that the docking of OCP on PB has a significant but transient impact on the structure of PB.

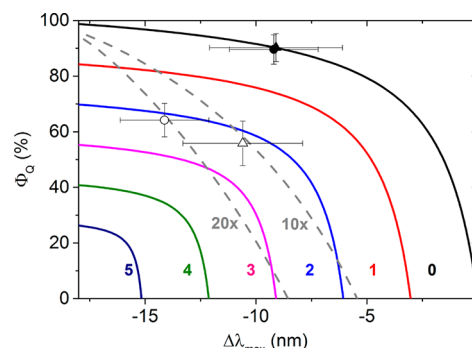


Figure 3. Docking of OCP^r decreases connectivity between the rods and the core of PB. Calculated shift in the fluorescence spectral peak position of PB ($\Delta\lambda_{\max}$) for all possible degrees of fluorescence quenching (Φ_Q) induced by OCP^r for different types of decreased interaction between the rods and core of PB. Continuous lines represent models whereby the indicated number of rods were completely disconnected from the core (i.e., the energy-transfer rate to and from those rods was 0). Gray dashed lines represent models where all the rods remained connected to the core but the energy-transfer rates to and from the rods were all decreased by a factor of 10 or 20. The four-compartmental kinetic model for PB detailed in ref 13, was used and the 660 nm emitting component of the core was considered to be the site of OCP-induced quenching. Average parameters of the measured fully quenched states (filled symbols) and intermediate states (open symbols) of WT-OCP–PB (circles) and R155L-OCP–PB (triangles) are shown. Peak positions were obtained from Figures 2 and 5, considering only the blue spectral bands obtained from the fits. For the fully quenched states, Φ_Q was calculated from $1 - \tau_F/\tau_U$, where τ_U and τ_F are the lifetimes of the quenched state and the preceding fully unquenched state, respectively. For the intermediate states, Φ_Q was calculated similarly but using an intensity ratio instead of a lifetime ratio, considering the blue spectral band of the intermediate states. Error bars denote standard deviations obtained from the fits. For more information, see Supporting Modeling.

Interestingly, the emission spectrum of the intermediate state displays also a clear additional band with a maximum near 745 nm (Figure 2). This broad and strongly red shifted band most likely originates from an OCP-induced charge-transfer (CT) state in one of the phycobilins of PB.^{28,29} The CT state could be either induced by the interaction between (1) the phycobilin and the carotenoid of OCP, (2) the phycobilin and amino acid residues of OCP, (3) OCP and the amino acid residues of PB, which in turn interact with the phycobilin, or (4) a combination of these three scenarios.

The emission spectra of the unquenched and fully quenched states with average fluorescence peak positions at 669.9 and 658.5 nm, respectively, resemble the bulk spectra reported previously,¹ as well as the single-molecule spectra of unquenched states.¹³ The red band present in the spectrum of the intermediate state is no longer visible in the fully quenched state. The large blue shift upon OCP-induced quenching is larger than any other spectral shift observed for the light-induced dynamics.¹³

The OCP-related energy quenching mechanism is switched off when cells are no longer exposed to high light intensity. The process of fluorescence recovery usually depends on FRP. Use of R155L-OCP in this study to induce energy quenching at the level of individual PBs allowed us to observe and investigate the recovery of fluorescence at the level of individual PBs, in the absence of FRP. When illuminating PB with blue light in the presence of R155L-OCP, the PB fluorescence intensity was

observed to decrease and the fluorescence lifetimes were found to shorten by 90% (down to 0.15 ± 0.01 ns, vide infra), similarly as in the presence of WT-OCP. However, in contrast to WT-OCP, in this case, the fluorescence recovered from the quenched state (Figure 4A,B). The concomitant increase in the

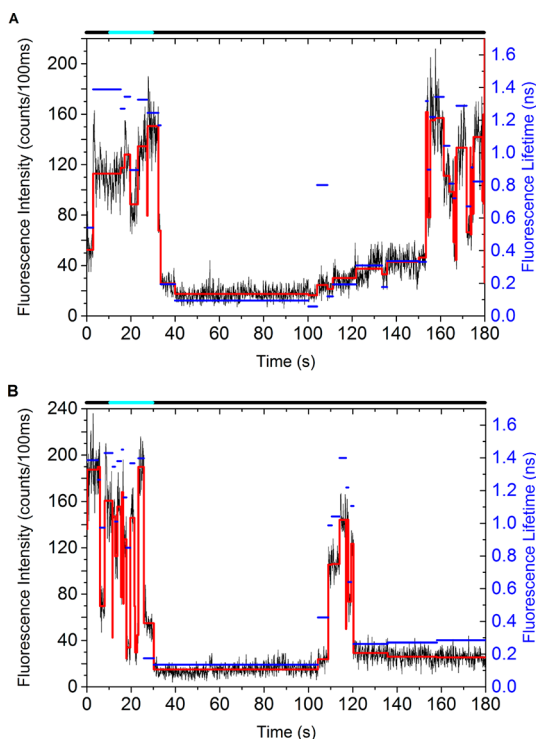


Figure 4. R155L-OCP induces reversible energy quenching of individual PBs. Two representative traces of binned fluorescence counts (black), resolved intensity levels (red), and associated fluorescence lifetimes (blue). Upon illumination (cyan bar on top) fluorescence quenching was induced. The PB in (a) remained quenched for ~ 120 s before the emission recovered. The complex in (b) initially entered the quenched state for ~ 80 s and recovered briefly via a short intermediate state. After 120 s, the fluorescence of PB was quenched again and remained quenched until the end of measurement. Complexes in (a) and (b) stayed intact during the entire measurement of 180 s. An irradiance of ~ 1.5 W/cm² was used to excite the PBs at 594 nm. Fluorescence lifetimes were fitted for intensity levels consisting of >500 photons.

fluorescence intensity and lifetime signifies the detachment of R155L-OCP from PB. A similar recovery of fluorescence after energy quenching induced by R155L-OCP was previously observed in bulk measurements,¹⁹ where it was directly related to the detachment of OCP from the complex.

Fluorescence emission spectra of PB before and after R155L-OCP-induced quenching were nearly indistinguishable (Figure 5A), confirming that interaction with OCP does not induce any permanent (i.e., preserved after the detachment of OCP) changes in the PB structure and spectral properties. Moreover, intermediate states with a clear, broad, red-shifted band were also observed in the presence of R155L-OCP, both for fluorescence quenching and recovery, suggesting that OCP docking and undocking mechanisms are involved in the induction of energy quenching and in recovery from the quenched state, respectively (Figure 5B).

Modeling of the relationship between Φ_Q and $\Delta\lambda_{\max}$ indicates that the connectivity between the core and rods is

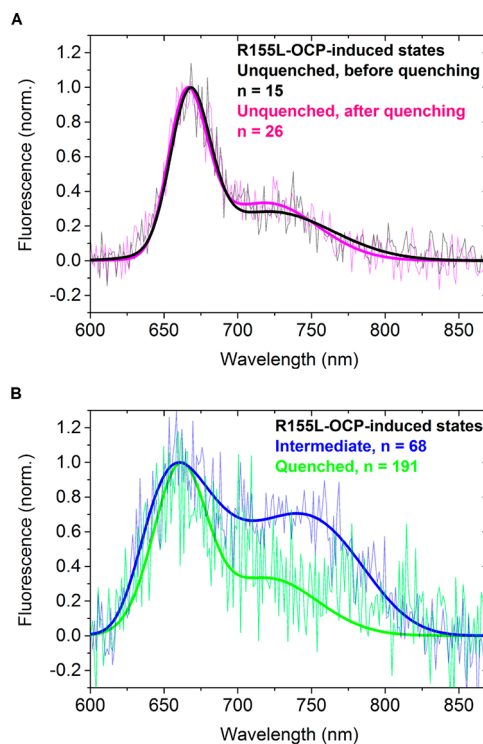


Figure 5. Interaction between OCP and PB does not introduce permanent changes in the PBs. Thin lines denote normalized fluorescence spectra and thick lines fitted double skewed Gaussians. (a) The difference between the spectrum of the unquenched states before (black) and after (magenta) quenching is negligible. (b) The difference between the spectra of the quenched (green) and intermediate (blue) states is mainly in the red part of the spectra. The blue band of the intermediate state's spectrum peaks at 657.5 ± 2.7 nm while that of the fully quenched state peaks at 658.6 ± 3.0 nm. The number of single-molecule spectra over which averaging was done is denoted by n . In all cases a measured baseline was subtracted from the spectra.

again significantly reduced when R155L-OCP–PB is in an intermediate state compared to its quenched and unquenched states (Figure 3). In fact, the experimental data point of the average intermediate state (open triangle) agrees well with a model where an average of two rods are transiently uncoupled, similarly to WT-OCP–PB, or where the energy-transfer rates between the core and all of the rods are on average 10–20 times slower than those for the quenched and unquenched states.

The fluorescence lifetime distribution obtained from all quenched states was investigated more closely. Quenched states, either photoactivated, available intrinsically for PBs in the absence of OCP, or induced by WT-OCP or R155L-OCP, revealed some interesting mechanistic insights into the OCP-induced mechanism (Figure 6). The OCP-induced quenched states are characterized by shorter fluorescence lifetimes than those that were light-induced and intrinsic for PB in the absence of OCP. Shorter fluorescence lifetimes mean that when OCP^r is bound to a PB more energy is dissipated than in the quenched states that are intrinsically available for PBs, per given time. The average fluorescence lifetime of 0.16 ns of PB in the OCP-induced quenched state corresponds remarkably well with the lifetime of 0.157 ns obtained in a previous bulk in vitro time-resolved fluorescence study, where a quenching rate of 30.3 ns^{-1} was calculated.¹⁵ It was shown that this quenching

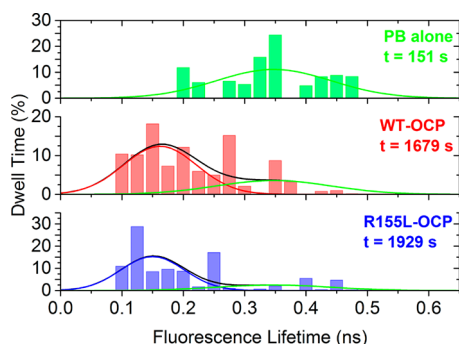


Figure 6. Without OCP, PBs do not enter fully quenched states. Distributions of fluorescence lifetimes shorter than 0.5 ns, weighted by their corresponding dwell times, for PB (green), induced by WT-OCP (red) and induced by R155L-OCP (blue). First, a Gaussian was fitted to the distribution for PB (green), and subsequently two Gaussians were fitted to the distributions of the OCP-induced quenched states. The lifetimes related to the activity of OCP were disentangled from the lifetimes of quenched states accessible by PBs in the absence of OCP by constraining the peak position and fwhm of the second Gaussian (green) to be the same as that of PB (top). Peak positions of these fits at 0.35 ± 0.03 (green), 0.16 ± 0.02 (red) and 0.15 ± 0.01 ns (blue) were taken as the average fluorescence lifetimes. The total dwell time considered is denoted by t .

rate strongly competes with excitation energy transfer to the photosystems (rate of 15.9 ns^{-1}),¹⁴ in particular, to Photosystem II (rate of 50 ns^{-1}),³⁰ allowing OCP to provide photoprotection to photosynthetic RCs.

By combining isolated PBs, OCP, and illumination, we were able to control the fluorescence emission from individual PB complexes. A biological system, composed of an engineered OCP–PB hybrid, using light for precise and reversible molecular control of the activation or deactivation of emitters is a promising candidate to contribute to the development of novel super-resolution imaging techniques where the emission from the fluorophores could be switched on and off.

We managed to control the interaction between OCP and individual PBs—two physiological partners—and revealed hidden molecular details of the crucial, photoprotective mechanism of cyanobacteria. Binding of OCP involves temporary rearrangements in the structure of PB, leading to decreased energy transfer from some of the rods to the core. Importantly, in the fully quenched state, the connectivity is regained and the whole complex, containing all of the rods, is in an energy-dissipating, quenched state. OCP in a complex with a PB stabilizes the latter and conserves its light harvesting functionality over prolonged periods of time.

The spectra of intermediate states suggest additionally that OCP induces directly or indirectly CT states in a phycobilin in PB. The involvement of these states in quenching needs to be further explored.

Thanks to R155L-OCP, we observed the complete cycle of the OCP-related mechanism, involving quenching and recovery from the quenched state, at the level of a single PB complex. Recovery of fluorescence after quenching shows that OCP-induced quenching is completely reversible and that the spectroscopic properties of PB are the same before and after quenching.

The interactions revealed in this study at the level of single molecules not only provide important insights into the dynamic molecular mechanisms in the photosynthetic apparatus of cyanobacteria but also constitute a new class of molecular

fluorescence markers in which emission can be manually controlled at the single-complex level.

EXPERIMENTAL METHODS

Sample Preparation. PBs were isolated in 0.8 M K-phosphate, pH 7.5 buffer from WT *Synechocystis* PCC 6803, as described previously.¹ Introduction of the point mutation in the OCP encoding gene was described elsewhere.¹⁹ WT-OCP and R155L-OCP were isolated from *Synechocystis* PCC 6803 ΔcrtR ³¹ and the R155L- ΔcrtR ¹⁹ mutant, respectively, as described elsewhere.¹⁸ All samples were stored in darkness at -80°C and thawed directly before measurement.

Experimental Conditions and Procedures. The PBs were prepared for the SMS measurement as described previously.¹³ Briefly, PBs diluted with 0.8 M K-phosphate, pH 7.5 buffer to $\sim 5 \text{ pmol}$ were immobilized on a poly-L-lysine-treated microscope glass and rinsed three times with the same buffer to remove unbound complexes.¹³ Thereafter, OCP was added to a final concentration of $2.1 \text{ }\mu\text{mol}$. The OCP initially saturated the surface of the coverslip, and the remaining fraction was freely diffusing. In order to induce photoconversion of OCP, the surface of the coverslip glass was illuminated for 20 s with $240 \text{ }\mu\text{mol}$ of blue photons $\text{s}^{-1} \text{ m}^{-2}$ emitted by a 475 nm LED. PBs were excited using an irradiance of $\sim 0.86 \text{ W/cm}^2$ at 594 nm, unless stated differently. The same objective was used to focus the excitation beam and collect the emitted fluorescence. Fluorescence intensity, lifetimes, and spectra were measured simultaneously after dividing the fluorescence beam by a 50/50 beam splitter, as described elsewhere.¹³ Blue light was removed from the beam by a combination of the three optical filters KC13, OC12, and XC18 (Utrex Cryostats, Estland).

In order to create the images shown in Figures S1 and S2, a window of $10 \text{ }\mu\text{m} \times 10 \text{ }\mu\text{m}$ was raster-scanned by the laser beam with a dwell time of 3 ms per pixel.

All measurements were performed in the presence of oxygen and at room temperature.

Data Analysis. Analysis of fluorescence intensity was performed using a home-written MatLAB (Mathworks) script based on the intensity change point algorithm described in ref 32, and the fluorescence lifetimes were fitted using code obtained from and described in ref 33. For intensity levels consisting of more than 500 photons, fluorescence lifetimes were resolved by fitting a monoexponential convolved with the measured IRF of the single-photon avalanche photodiode. Kinetic modeling was performed in Wolfram Mathematica. Analyzed data was visualized using Origin 9.1.

ASSOCIATED CONTENT

Supporting Information

The Supporting Information is available free of charge on the ACS Publications website at DOI: 10.1021/acs.jpclett.8b00767.

Supporting figures showing fluorescence quenching under various conditions, fluorescence traces, and dwell times, supporting modeling, and supporting references (PDF)

AUTHOR INFORMATION

Corresponding Author

*E-mail: gwizdala.michal@gmail.com. Phone: +27607175821.

ORCID

Michal Gwizdala: 0000-0002-3509-6554

Tjaart P. J. Krüger: 0000-0002-0801-6512

Author Contributions

All authors have given approval to the final version of the manuscript. M.G., T.P.J.K., D.K., and R.v.G. designed the research. A.W. and M.G. isolated the samples. M.G. did the measurements on a setup built by T.P.J.K. M.G., J.L.B., and T.P.J.K. analyzed the data and interpreted the results. M.G. wrote the manuscript with help from T.P.J.K. All authors had editorial input on the article.

Notes

The authors declare no competing financial interest.

ACKNOWLEDGMENTS

The authors would like to thank Michael Gruber, Lijin Tian, and Bart van Oort for fruitful discussions. M.G. acknowledges funding from the European Molecular Biology Organisation (EMBO) via a Long-Term Fellowship and from the Claude Leon Foundation via a Postdoctoral Fellowship. J.L.B. was supported by the VU University Amsterdam–NRF South Africa Desmond Tutu Programme. The work of M.G., T.P.J.K., and R.v.G. was supported by an advanced investigator grant (267333, PHOTPROT) from the European Research Council. R.v.G. gratefully acknowledges his “Academy Professor” grant from the Royal Netherlands Academy of Arts and Sciences (KNAW). The work of A.W. and D.K. was supported by the Agence Nationale de la Recherche (Project CYANOPROTECT), the Centre National de la Recherche Scientifique (CNRS), the Commissariat à l’Energie Atomique (CEA), the HARVEST EU FP7 Marie Curie Research Training Network, Phycosource, and the French Infrastructure for Integrated Structural Biology (Grant ANR-10-INSB-05-01). T.P.J.K. was supported by the National Equipment Programme of the National Research Foundation (NRF) (Grant N00500, Project 87990), the NRF Thuthuka programme (Grant N00726, Project 94107), and the Photonics Initiative of South Africa.

REFERENCES

- (1) Gwizdala, M.; Wilson, A.; Kirilovsky, D. In Vitro Reconstitution of the Cyanobacterial Photoprotective Mechanism Mediated by the Orange Carotenoid Protein in *Synechocystis* PCC 6803. *Plant Cell* **2011**, *23* (7), 2631–2643.
- (2) Kirilovsky, D.; Kerfeld, C. A. Cyanobacterial Photoprotection by the Orange Carotenoid Protein. *Nat. Plants* **2016**, *2* (12), 16180.
- (3) Sluchanko, N. N.; Slonimskiy, Y. B.; Maksimov, E. G. Features of Protein–protein Interactions in the Cyanobacterial Photoprotection Mechanism. *Biochemistry* **2017**, *82* (13), 1592–1614.
- (4) Wilson, A.; Ajlani, G.; Verbavatz, J.; Vass, I.; Kerfeld, C.; Kirilovsky, D. A Soluble Carotenoid Protein Involved in Phycobilisome-Related Energy Dissipation in Cyanobacteria. *Plant Cell* **2006**, *18* (4), 992–1007.
- (5) *Non-Photochemical Quenching and Energy Dissipation in Plants, Algae and Cyanobacteria*; Demmig-Adams, B., Garab, G., Adams, W., III, Govindjee, Eds.; Advances in Photosynthesis and Respiration; Springer Netherlands: Dordrecht, The Netherlands, 2014; Vol. 40.
- (6) Glazer, A. N. Phycobilisome: A Macromolecular Complex Optimized for Light Energy Transfer. *Biochim. Biophys. Acta, Rev. Bioenerg.* **1984**, *768* (1), 29–51.
- (7) MacColl, R. Cyanobacterial Phycobilisomes. *J. Struct. Biol.* **1998**, *124* (2–3), 311–334.
- (8) Adir, N. Elucidation of the Molecular Structures of Components of the Phycobilisome: Reconstructing a Giant. *Photosynth. Res.* **2005**, *85* (1), 15–32.
- (9) Watanabe, M.; Ikeuchi, M. Phycobilisome: Architecture of a Light-Harvesting Supercomplex. *Photosynth. Res.* **2013**, *116* (2–3), 265–276.

- (10) Lundell, D. J.; Glazer, A. N. Molecular Architecture of a Light-Harvesting Antenna. Structure of the 18 S Core-Rod Subassembly of the *Synechococcus* 6301 Phycobilisome. *J. Biol. Chem.* **1983**, *258* (2), 894–901.
- (11) Bar-Eyal, L.; Eisenberg, I.; Faust, A.; Raanan, H.; Nevo, R.; Rappaport, F.; Krieger-Liszka, A.; Sétif, P.; Thurotte, A.; Reich, Z.; et al. An Easily Reversible Structural Change Underlies Mechanisms Enabling Desert Crust Cyanobacteria to Survive Desiccation. *Biochim. Biophys. Acta, Bioenerg.* **2015**, *1847* (10), 1267–1273.
- (12) Eisenberg, I.; Caycedo-Soler, F.; Harris, D.; Yochelis, S.; Huelga, S. F.; Plenio, M. B.; Adir, N.; Keren, N.; Paltiel, Y. Regulating the Energy Flow in a Cyanobacterial Light-Harvesting Antenna Complex. *J. Phys. Chem. B* **2017**, *121* (6), 1240–1247.
- (13) Gwizdala, M.; Berera, R.; Kirilovsky, D.; van Grondelle, R.; Krüger, T. P. J. Controlling Light Harvesting with Light. *J. Am. Chem. Soc.* **2016**, *138* (36), 11616–11622.
- (14) Tian, L.; van Stokkum, I. H. M.; Koehorst, R. B. M.; Jongerijs, A.; Kirilovsky, D.; van Amerongen, H. Site, Rate, and Mechanism of Photoprotective Quenching in Cyanobacteria. *J. Am. Chem. Soc.* **2011**, *133* (45), 18304–18311.
- (15) Tian, L.; Gwizdala, M.; van Stokkum, I. H. M.; Koehorst, R. B. M.; Kirilovsky, D.; van Amerongen, H. Picosecond Kinetics of Light Harvesting and Photoprotective Quenching in Wild-Type and Mutant Phycobilisomes Isolated from the Cyanobacterium *Synechocystis* PCC 6803. *Biophys. J.* **2012**, *102* (7), 1692–1700.
- (16) Jallet, D.; Gwizdala, M.; Kirilovsky, D. ApcD, ApcF and ApcE Are Not Required for the Orange Carotenoid Protein Related Phycobilisome Fluorescence Quenching in the Cyanobacterium *Synechocystis* PCC 6803. *Biochim. Biophys. Acta, Bioenerg.* **2012**, *1817* (8), 1418–1427.
- (17) van Stokkum, I. H. M.; Gwizdala, M.; Tian, L.; Snellenburg, J. J.; van Grondelle, R.; van Amerongen, H.; Berera, R. A Functional Compartmental Model of the *Synechocystis* PCC 6803 Phycobilisome. *Photosynth. Res.* **2018**, *135* (1–3), 87–102.
- (18) Wilson, A.; Punginelli, C.; Gall, A.; Bonetti, C.; Alexandre, M.; Routaboul, J.; Kerfeld, C.; van Grondelle, R.; Robert, B.; Kennis, J.; et al. A Photoactive Carotenoid Protein Acting as Light Intensity Sensor. *Proc. Natl. Acad. Sci. U. S. A.* **2008**, *105* (33), 12075–12080.
- (19) Wilson, A.; Gwizdala, M.; Mezzetti, A.; Alexandre, M.; Kerfeld, C. A.; Kirilovsky, D. The Essential Role of the N-Terminal Domain of the Orange Carotenoid Protein in Cyanobacterial Photoprotection: Importance of a Positive Charge for Phycobilisome Binding. *Plant Cell* **2012**, *24* (5), 1972–1983.
- (20) Leverenz, R. L.; Sutter, M.; Wilson, A.; Gupta, S.; Thurotte, A.; Bourcier de Carbon, C.; Petzold, C. J.; Ralston, C.; Perreau, F.; Kirilovsky, D.; et al. A 12 Å Carotenoid Translocation in a Photoswitch Associated with Cyanobacterial Photoprotection. *Science* **2015**, *348* (6242), 1463–1466.
- (21) Liu, H.; Zhang, H.; Orf, G. S.; Lu, Y.; Jiang, J.; King, J. D.; Wolf, N. R.; Gross, M. L.; Blankenship, R. E. Dramatic Domain Rearrangements of the Cyanobacterial Orange Carotenoid Protein upon Photoactivation. *Biochemistry* **2016**, *55* (7), 1003–1009.
- (22) Harris, D.; Tal, O.; Jallet, D.; Wilson, A.; Kirilovsky, D.; Adir, N. Orange Carotenoid Protein Burrows into the Phycobilisome to Provide Photoprotection. *Proc. Natl. Acad. Sci. U. S. A.* **2016**, *113* (12), E1655–E1662.
- (23) Boulay, C.; Wilson, A.; D’Haene, S.; Kirilovsky, D. Identification of a Protein Required for Recovery of Full Antenna Capacity in OCP-Related Photoprotective Mechanism in Cyanobacteria. *Proc. Natl. Acad. Sci. U. S. A.* **2010**, *107* (25), 11620–11625.
- (24) Gwizdala, M.; Wilson, A.; Omairi-Nasser, A.; Kirilovsky, D. Characterization of the *Synechocystis* PCC 6803 Fluorescence Recovery Protein Involved in Photoprotection. *Biochim. Biophys. Acta, Bioenerg.* **2013**, *1827* (3), 348–354.
- (25) Sutter, M.; Wilson, A.; Leverenz, R. L.; Lopez-Igual, R.; Thurotte, A.; Salmeen, A. E.; Kirilovsky, D.; Kerfeld, C. A. Crystal Structure of the FRP and Identification of the Active Site for Modulation of OCP-Mediated Photoprotection in Cyanobacteria. *Proc. Natl. Acad. Sci. U. S. A.* **2013**, *110* (24), 10022–10027.

- (26) Sluchanko, N. N.; Klementiev, K. E.; Shirshin, E. A.; Tsoraev, G. V.; Friedrich, T.; Maksimov, E. G. The Purple Trp288Ala Mutant of *Synechocystis* OCP Persistently Quenches Phycobilisome Fluorescence and Tightly Interacts with FRP. *Biochim. Biophys. Acta, Bioenerg.* **2017**, 1858 (1), 1–11.
- (27) Andreoni, A.; Lin, S.; Liu, H.; Blankenship, R. E.; Yan, H.; Woodbury, N. W. Orange Carotenoid Protein as a Control Element in an Antenna System Based on a DNA Nanostructure. *Nano Lett.* **2017**, 17 (2), 1174–1180.
- (28) Romero, E.; Mozzo, M.; van Stokkum, I. H. M.; Dekker, J. P.; van Grondelle, R.; Croce, R. The Origin of the Low-Energy Form of Photosystem I Light-Harvesting Complex Lhca4: Mixing of the Lowest Exciton with a Charge-Transfer State. *Biophys. J.* **2009**, 96 (5), L35–37.
- (29) Krüger, T. P. J.; Novoderezhkin, V. I.; Iliaia, C.; van Grondelle, R. Fluorescence Spectral Dynamics of Single LHCII Trimers. *Biophys. J.* **2010**, 98 (12), 3093–3101.
- (30) Acuña, A. M.; Van Alphen, P.; van Grondelle, R.; van Stokkum, I. H. M. The Phycobilisome Terminal Emitter Transfers Its Energy with a Rate of $(20 \text{ ps})^{-1}$ to Photosystem II. *Photosynthetica* **2018**, 56, 265–274.
- (31) Wilson, A.; Punginelli, C.; Couturier, M.; Perreau, F.; Kirilovsky, D. Essential Role of Two Tyrosines and Two Tryptophans on the Photoprotection Activity of the Orange Carotenoid Protein. *Biochim. Biophys. Acta, Bioenerg.* **2011**, 1807 (3), 293–301.
- (32) Watkins, L. P.; Yang, H. Detection of Intensity Change Points in Time-Resolved Single-Molecule Measurements. *J. Phys. Chem. B* **2005**, 109 (1), 617–628.
- (33) Enderlein, J.; Erdmann, R. Fast Fitting of Multi-Exponential Decay Curves. *Opt. Commun.* **1997**, 134 (1), 371–378.